Sol–gel TiO_2–SiO_2 films as protective coatings against corrosion of 316L stainless steel in H_2SO_4 solutions

M. ATIK, P. DE LIMA NETO, M. A. AEGERTER, L. A. AVACA*

Instituto de Física e Química de São Carlos, Universidade de São Paulo, C. P. 369 - 13560-970, São Carlos, SP, Brazil

Sol–gel TiO_2–SiO_2 films were deposited on 316L stainless steel by dip coating process from a sono-catalysed sol of composition $30TiO_2$–$70SiO_2$ prepared from a mixture of $Ti(OC_2H_5)_4$ and $Si(OC_2H_5)_4$, absolute ethanol C_2H_5OH and glacial acetic acid CH_3COOH as precursors and solvents. The films, densified at 800° C in air for 2 h, are composed of small orthorhombic titania (anatase) crystallites embedded in a SiO_2 amorphous matrix as identified by X-ray diffraction. The temperature dependence of the film morphology was observed using scanning electron microscopy (SEM) and the content was determined by FTIR reflection spectroscopy. The corrosion behaviour of 316L stainless steel samples coated with densified $30TiO_2$–$70SiO_2$ films was studied in 15% H_2SO_4 by potentiodynamic polarization curves at 25, 40 and 50° C. The measured corrosion rates show a considerable decrease for the protected steel samples in comparison to the bare substrate. The effect of time of heat treatment of the films on the corrosion parameters is also reported.

1. Introduction

Inorganic coatings having a vitreous structure have been widely used as protective coatings for stainless steel (SS) and other metals and alloys [1–3]. These coatings improve the chemical and physical properties of the metal surfaces relative to corrosion, friction and wear without altering the original properties of strength and toughness of the substrates. The application of these coatings is usually an involved process adding to the final cost of the material.

In recent years sol–gel methods have been developed for the deposition of a variety of oxide materials on metals and other surfaces [4, 5]. The chemical processing and technical applications of sol–gel films have been recently reviewed by Schmidt [6] and by Sakka and Yoko [7], respectively. The method involves the preparation of sols containing the metal compounds in the form of metal alkoxides or acetylacetonates, inorganic salts, etc., dissolved in alcohols and water as hydrolysis agents. The films can be deposited by spin, dip, spray coating or electrophoresis. These processes can be repeated allowing the possibility of obtaining thick coatings (up to 1–2 μm) even on very large surfaces and on one or both sides of the substrates. The films obtained in this manner are usually wet, amorphous and porous and contain still a large amount of organic compounds. The films are dried at around 100° C and the organic compounds are eliminated typically at around 350–450° C by heat treatment in air. The porosity can be controlled by heat treatments at relatively low temperatures and complete densification is usually obtained at temperatures around the vitreous transition temperature of the materials, T_g. The sol–gel methods offer therefore potential advantages over traditional techniques.

The preparation and characterization of sol–gel films having specific chemical function have been scarcely studied. Al_2O_3 [8], Si–O–N, Si_3N_4 [9, 10] films have been proposed for semiconductor passivation. SiO_2 [11] and TiO_2–SiO_2 [12] are known to prevent alkali diffusion. The prevention of chemical corrosion and oxidation of mild steel, carbon steel and stainless steels has been tested with SiO_2 [13], SiO_2–B_2O_3 [14, 15], mullite ($2SiO_2$–$3Al_2O_3$) [16], ZrO_2 [17–19], SiO_2 (modified by polyfluoroalkoxysilane, water and oil repellent) [20], TiO_2–SiO_2 [21] and more recently with ZrO_2–CeO_2 and TiO_2–CeO_2 [22] coatings. They increase the protection of metal substrates from air corrosion (tested up to 800° C) and acid attack (tested up to 80° C). The most promising prevention for stainless steel (SS) has been so far reported by our group using sol–gel films of ZrO_2 where this property has been studied by electrochemical techniques in NaCl [23] and H_2SO_4 [24] solutions. Some preliminary results for SiO_2, TiO_2–SiO_2, SiO_2–Al_2O_3 in H_2SO_4 solutions have also been reported [25]. In all cases, the films were prepared by dip-coating using sonocatalysed sols [26].

In this work, the preparation of TiO_2–SiO_2 films deposited on 316L SS and potentiodynamic studies of the corrosion behaviour of the samples in deaerated 15% H_2SO_4 solutions at 25, 40 and 50° C are fully described. The effect of different heat treatments on the behaviour of the coated samples is also studied.

* Author to whom correspondence should be addressed.

2. Experimental details

2.1. *Substrate*

The substrate used was 316L stainless steel of composition (wt %): 67.25 Fe, 18.55 Cr, 11.16 Ni, 2.01 Mo, 0.026 Cu, 0.15 Si and 0.028 C. Samples (3.0 cm × 1.5 cm × 0.1 cm) were mechanically cut from large foils and then degreased ultrasonically in acetone. This material was chosen taking into account the heat treatment necessary for the densification of the coatings (see below). Therefore, a low carbon content steel was judged more convenient since it is less susceptible to sensitization which in turn might promote an enhanced corrosion [2]. In addition, 316L SS is a material widely used in chemical industry environments [27].

2.2. *Preparation of the films*

$Ti(OC_2H_5)_4$ and $Si(OC_2H_5)_4$ were used as sources of titania and silica. The sol was prepared at room temperature by dissolving the alkoxides in absolute ethanol C_2H_5OH (0.43 mol of absolute ethanol per mol of alkoxide) to which was added 0.087 mol of acetic acid CH_3OOH. The composition of the solution was $30TiO_2$–$70SiO_2$ (mol %).

The mixture was submitted to intense ultrasonic radiation (20 kHz) produced by a Heat Systems Ultrasonics W 385 sonicator. After 25 min the liquid became homogeneous and clear and remained stable for about five weeks at room temperature when kept in a close vessel.

Coating of the substrates has been done by dip coating process, withdrawing the substrates from the solution at a constant rate of 10 cm min^{-1}. The gel films were dried at 60° C for 15 min and then densified in a furnace in an air atmosphere. The heat-treatment protocol for TiO_2–SiO_2 film preparations was the following: the temperature was raised at a rate of 5° C min^{-1} with isothermal holdings, first at 450° C for 1 h and then at 800° C for 2 h. The thickness of the heat treated films are typically 0.4–0.6 μm [21].

2.3. *Characterization of the films*

2.3.1. X-ray diffraction. Analysis of uncoated and coated substrates were made with a Philips diffractometer using CuK_α radiation. Figure 1(a) shows the diffractogram of 316L stainless steel as received where it is observed three distinct peaks at 0.208, 0.18 and 0.127 nm corresponding to the cubic phase of the alloy containing Cr, Fe and Ni.

When heated at 800° C the uncoated substrates present additional diffraction peaks with d values of 0.49, 0.36, 0.297, 0.267, 0.253, 0.153, 0.169 and 0.149 nm. The crystalline phases formed were a mixture of cubic and hexagonal Cr_2O_3 and tetragonal Cr_3O_4 (Fig. 1(b)).

Besides the three diffraction peaks of SS, the substrate coated with $30TiO_2$–$70SiO_2$ films heated at 800° C in air for 2 h showed additional peaks with $d = 0.276$, 0.230 and 0.131 nm corresponding to orthorhombic titania (anatase) [21]; as no change was observed in the relative intensity of the peaks of the alloy, it can be concluded that no oxidation of the coated samples has occurred during the heat treatment (Fig. 1(c)).

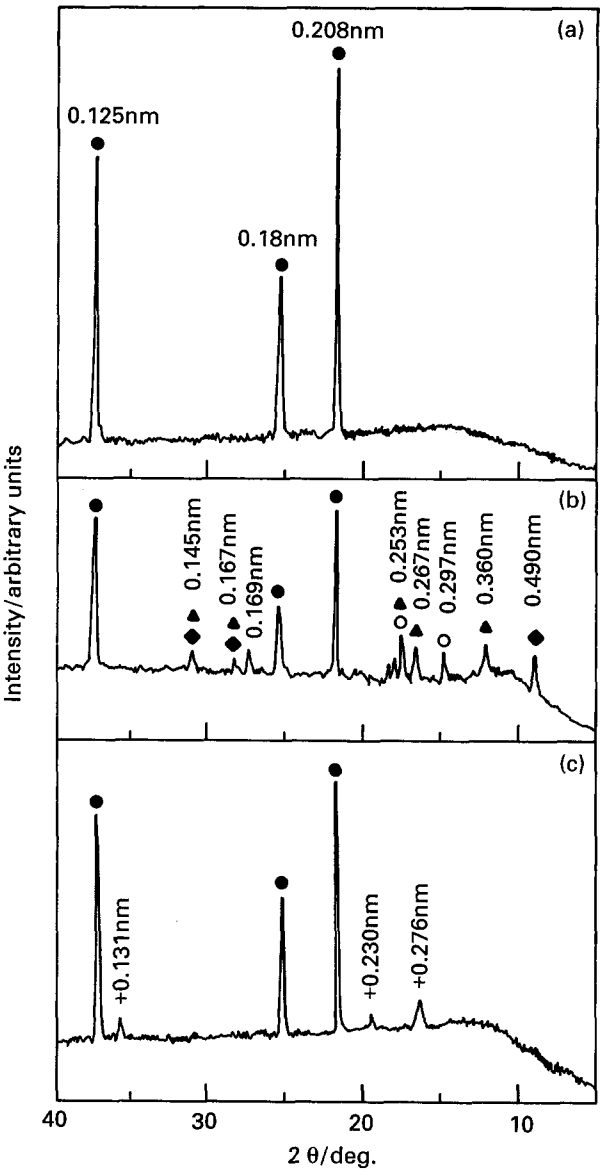

Fig. 1. XRD patterns of uncoated and coated substrates (a) 316L SS as received; (b) 316L SS treated at 800° C during 2 h; (●) SS, (○) cubic Cr_2O_3, (▲) hexagonal Cr_2O_3 (◆) tetragonal Cr_3O_4; (c) coated sample with $30TiO_2$–$70SiO_2$ film heat treated at 800° C in air for 2 h; (●) SS, (+) TiO_2 (anatase).

2.3.2. Infrared spectroscopy. A Bomen FTIR spectrometer was used to obtain high resolution spectra of the coatings in the 400–4000 cm^{-1} range; the measurements were obtained at room temperature by reflection at an incident angle of 30°.

Figure 2(a) shows the spectrum of a coating deposited on 316L stainless steel dried at 25° C. The band observed at 1070 cm^{-1} corresponds to the vibration of the asymmetric stretching mode of the Si–O band

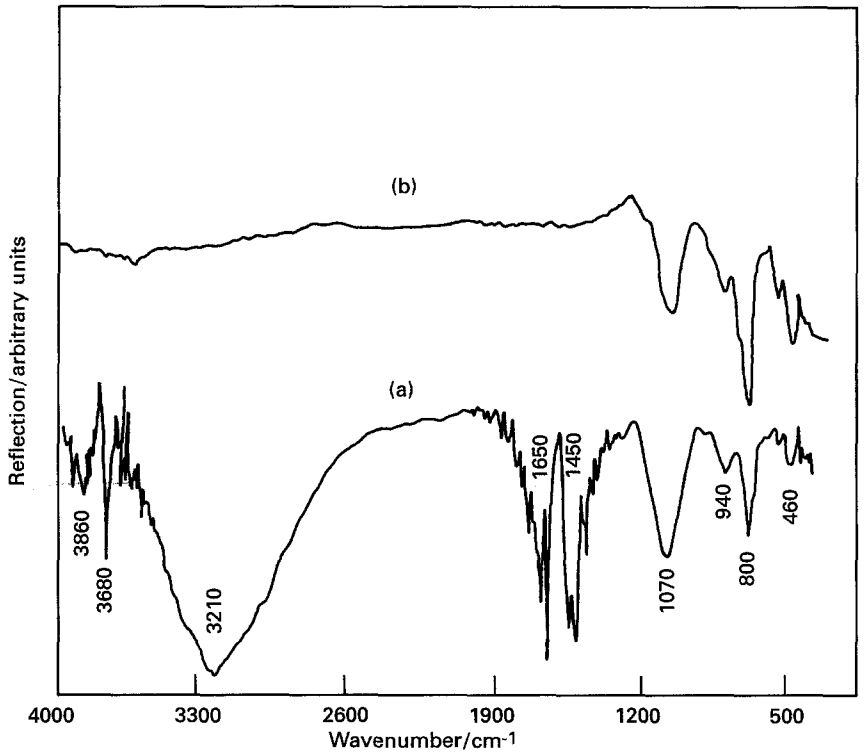

Fig. 2. IR spectra of $30TiO_2$–$70SiO_2$ films deposited on 316L stainless steel measured in reflection at an angle of 30° (a) dried at 25° C; (b) after heating in air at 800° C for 2 h.

and the shoulder on the high energy side is attributed to the symmetric vibration of the same bond. The well defined band at 800 cm^{-1} is linked to the ring structure while the band at 460 cm^{-1} is attributed to symmetric bond bending of O–Si–O [26]. The presence of bands at 1450 and 1650 cm^{-1} is attributed to vibration of Si–O–C and Ti–O–C molecules, respectively. The absorptions of the C–H and OH groups are observed near 3680–3860 cm^{-1} and 3210 cm^{-1}, respectively, while the bands at 940 and 680 cm^{-1} are attributed to the vibrations of Si–O–Ti.

After heating at 800° C for 2 h, the Si–O–Si and Si–O–Ti bands are better defined and the bands of CH, OH and mixtures of Si–O–C and Ti–O–C disappear completely (Fig. 2(b)).

2.3.3. Scanning electron microscopy (SEM). The morphology of the surface was examined by scanning electron microscopy (Jeol JSM–6300F and Zeiss 960). Figure 3(a) shows the texture of the stainless steel surface as received. After heat treatment of the sample for 2 h in air at 800° C small crystals grow at the surface in agreement with the XRD analysis (Fig. 3(b)). Figure 3(c) shows the micrograph of a thin film $30TiO_2$–$70SiO_2$ deposited on 316L SS and heated in air at 800° C for 2 h. The resulting coating is dense and homogeneous, without the appearance of cracks.

2.3.4. Electrochemical measurements. Electrochemical measurements were carried out in order to determine the potentiodynamic behaviour of samples in deaerated 15% H_2SO_4 (Merck p.a.) aqueous (Milli-Q) solutions at 25, 40 and 50° C. The working electrodes were 316L SS plates either bare or coated with $30TiO_2$–$70SiO_2$ of 0.4–0.6 μm thickness immersed 1 cm into the solution. Bare plates, heat-treated at 800° C for 2 h, were also used. Freshly prepared samples were used for each experiment. A saturated calomel electrode (SCE) was used as reference while a platinum foil served as the auxiliary electrode. A 273 PAR potentiostat linked to a microcomputer for data acquisition and handling through the 342 PAR corrosion measurement software was used for the experiments. The potentiodynamic measurements were initiated at −0.7 V vs SCE and scanned continuously in the anodic direction at 1 mV s^{-1}.

3. Results and discussion

Figures 4 to 6 show the potentiodynamic polarization curves for the different samples under examination in deaerated 15% H_2SO_4 solutions at 25, 40 and 50° C, respectively. The effect of the $30TiO_2$–$70SiO_2$ coating is noticeable in both the cathodic and the anodic branches of the curves. On the cathodic side, the slope for the hydrogen evolution reaction is about $2.3\,2RT/F$ (curves (a)), a value coherent with the common mechanisms accepted for this reaction, i.e. a Volmer–Heyrovsky sequence [28]. The value of the slope is maintained in the presence of the coating (curves (c)) suggesting that the mechanism remains unchanged; however the experimental points are shifted to lower values of the current density. These facts indicate that the coating is acting as a physical barrier which diminishes the active area for reaction by a factor which could be as high as 50 in some cases (Fig. 5). An intermediate behaviour is observed for the heat-treated samples without the coating (curves (b)), but this is difficult to interpret without a detailed knowledge of the processes occurring in the bulk structure as well as in the oxide layers of the SS during the heating.

The anodic branches of the polarization curves

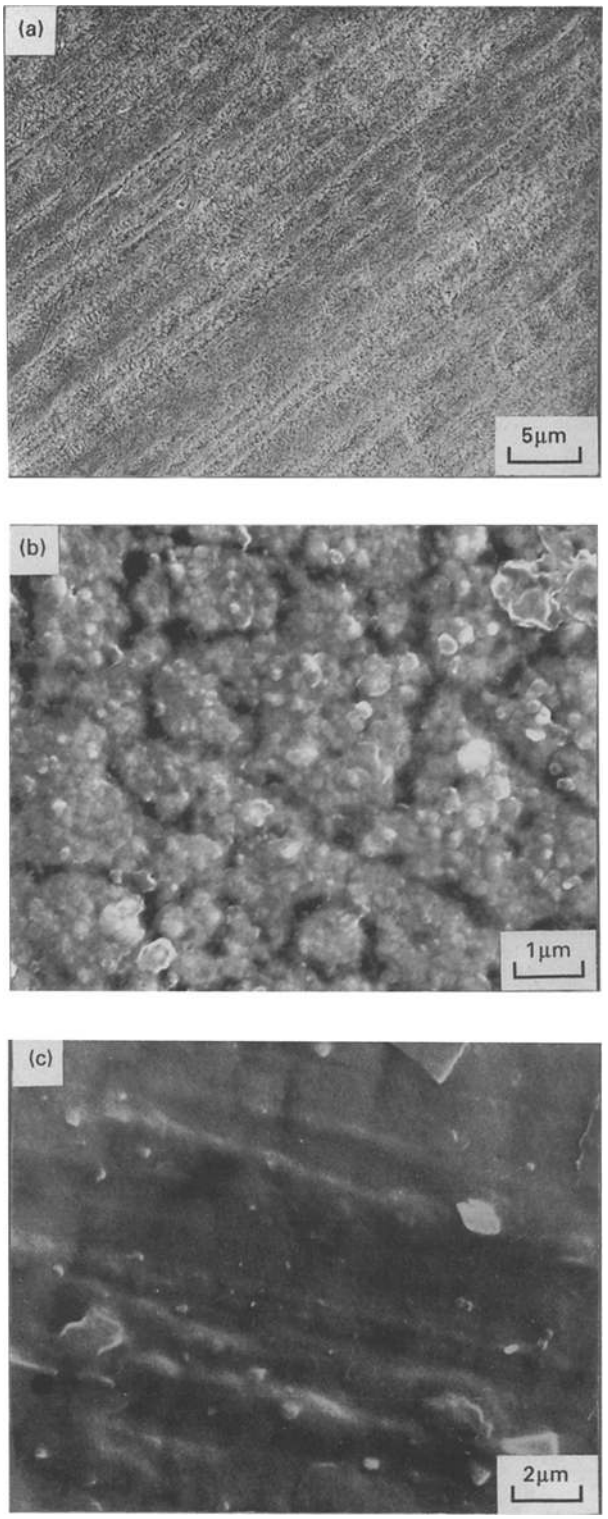

Fig. 3. SEM micrograph (a) 316L SS surface as received; (b) surface of 316L SS after oxidation in air at 800° C for 2 h; (c) micrograph of $30TiO_2$–$70SiO_2$ film deposited on 316L SS after heating in air at 800° C during 2 h.

(Figs 4 to 6) show that the coating has a strong effect on the current density in the passive region, diminishing its value by almost one order of magnitude. In the same region, the heat treated samples (curves (b)) show current densities somewhat higher than the untreated substrate (curves (a)) again revealing surface changes during the treatment.

The combined cathodic and anodic effects of the coatings on the corrosion behaviour of 316L SS can be visualized more clearly in Table 1, where the relevant corrosion parameters derived from Figs 4 to 6 are collected. Thus, although the presence of the film alters the value of the corrosion potential (E_{corr}) very little, the polarization resistance (R_p) increases considerably and the corrosion rate (CR) is dramatically reduced, in particular at 50° C. Even in relation to the heat treated samples, which seem to be more resistant to acid attack, the effect of the coating is still considerable again showing higher values of R_p.

Table 1. Electrochemical corrosion parameters derived from the polarization curves (Figs 4–6) obtained at 25, 40 and 50° C in deaerated 15% H_2SO_4

Sample	*T*/°C	$-E_{corr}$*/mV	R_p†/kΩ cm²	CR‡/mpy
	25	286	1.80	11.5
316L SS	40	261	0.37	35.2
	50	280	0.35	53.8
316L SS heat	25	306	1.45	5.0
treated at	40	304	0.57	19.8
800° C for 2 h	50	307	0.14	41.2
316L SS with	25	291	10.72	2.2
$30TiO_2$–$70SiO_2$	40	297	5.70	5.7
coating heat	50	293	3.10	6.3
treated at				
800° C for 2 h				

* Corrosion potential/mV vs SCE.
† Polarization resistance/kΩ cm².
‡ Corrosion rate/mills per year.

To assess better the influence of the coating structure on their protective properties against acid corrosion, comparative experiments were carried out at 25° C using $30TiO_2$–$70SiO_2$ films submitted to different heat treatments. For this, one sample was heated for 2 h at 600° C resulting in an essentially amorphous structure while the others were heat treated at 800° C for lengths of time varying from 2 to 20 h. Figure 7 shows the corresponding polarization curves obtained in 15% H_2SO_4 at room temperature while the relevant electrochemical parameters calculated for the samples are collected in Table 2.

The results of Table 2 suggest that the coatings heat treated at 600° C for 2 h offer apparently similar protection for SS against acid corrosion as those treated at 800° C. However the corresponding polarization

Table 2. Effect of heat treatment of the coating on the electrochemical corrosion parameters derived from the polarization curves (Fig. 7) and obtained in deaerated 15% H_2SO_4 at 25° C

Heat treatment/° C	*Time*/h	$-E_{corr}$*/mV	R_p†/kΩ cm²	CR‡/mpy
600	2	293	6.21	2.4
800	2	291	10.72	2.2
800	5	294	11.71	2.9
800	15	314	5.46	4.4
800	20	291	1.13	38.5

* Corrosion potential.
† Polarization resistance.
‡ Corrosion rate.

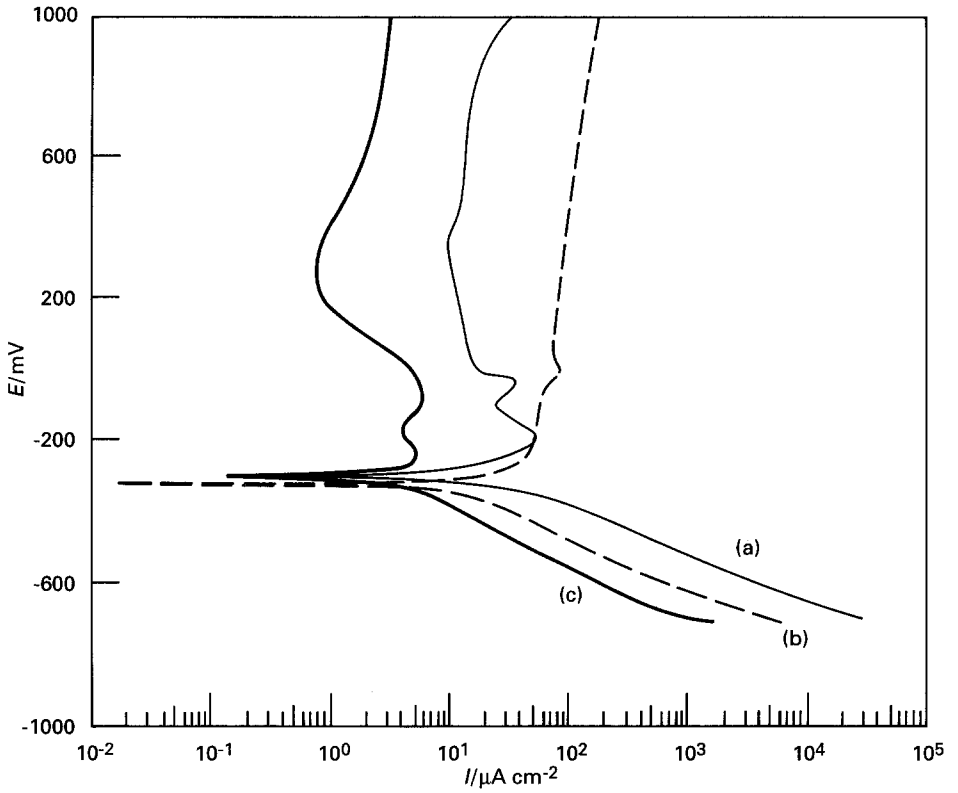

Fig. 4. Polarization curve recorded at 1 mV s^{-1} in deaerated 15% H_2SO_4 at 25° C (a) 316L SS as received; (b) 316L SS heat treated at 800° C for 2 h and (c) sample coated with $30TiO_2$–$70SiO_2$ treated at 800° C for 2 h. Potentials referred to SCE.

curve (Fig. 7) is not totally satisfactory, showing large values of the current density in the anodic branch. Furthermore, the heat treatment at 800° C was chosen after careful investigation of the physical properties of the coatings [21]. In particular, the $30TiO_2$–$70SiO_2$ coatings crystallize at ~ 650° C resulting in anatase crystallites in an amorphous silica matrix, which is a more stable structure. Therefore, it can be concluded that the best protection is obtained with the coatings treated at 800° C for 2 h.

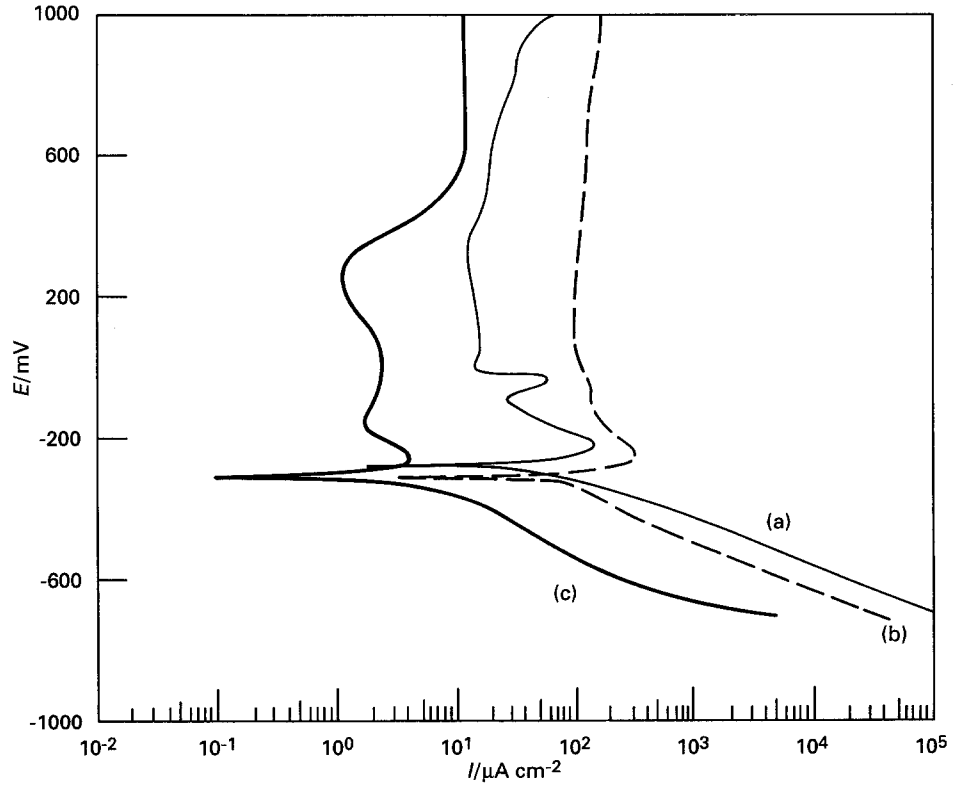

Fig. 5. Same as Fig. 4 but measured at 40° C.

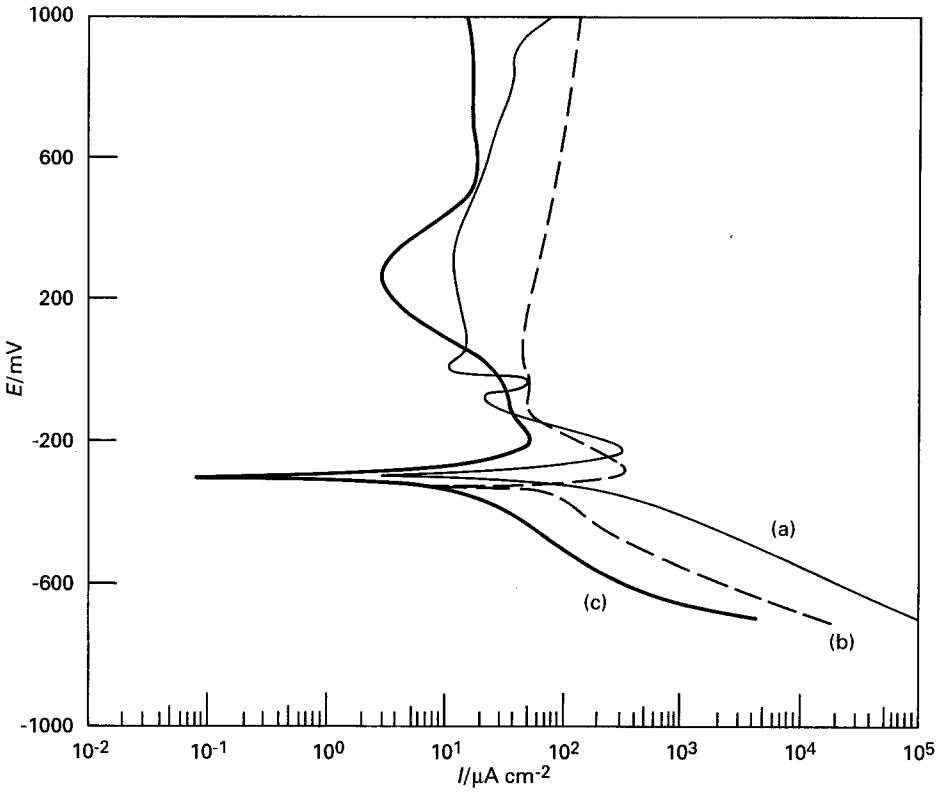

Fig. 6. Same as Fig. 4 but measured at 50° C.

As the heat treatment is prolonged to 15 h, the samples loose their protective ability to a small extent (Table 2). When the treatment is further extended to 20 h there is a dramatic change in properties and the samples show corrosion characteristics which are even worse than those of the base material (Tables 1 and 2). This behaviour is due to the occurrence of cracks in the film due to the growth of Cr_2O_3 at the SS/film interface. Previous studies of X-ray diffraction patterns of similar samples [21]

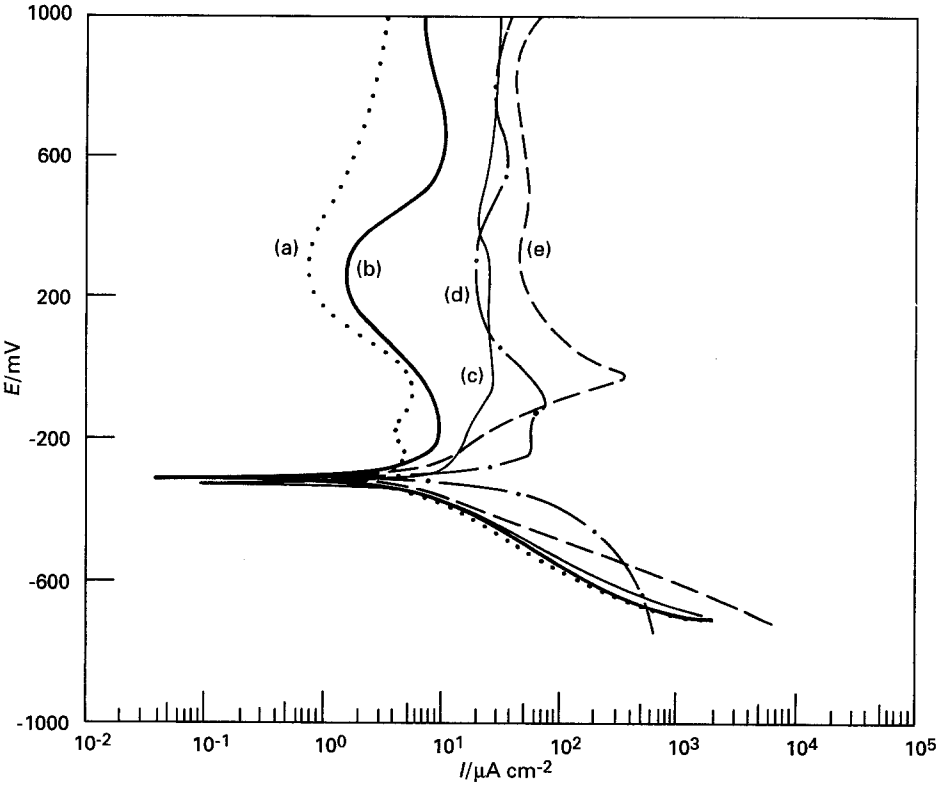

Fig. 7. Effect of heat treatment of the coatings on the polarization curve in deaerated 15% H_2SO_4 at 25° C. The curves correspond to $30TiO_2$–$70SiO_2$ films treated at 800° C for (a) 2 h, (b) 5 h, (c) 15 h and (d) 20 h and (e) 600° C for 2 h.

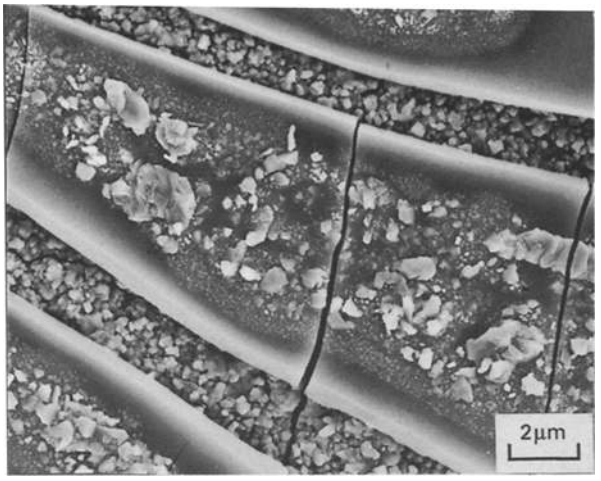

Fig. 8. SEM micrograph of film with cracks and small Cr_2O_3 crystals.

show little changes for heat-treatment at 800° C up to 15 h. For 20 h, there is clear evidence of the appearance of chromium oxide crystals. The growth of these crystals from the base material breaks the coating, leaving an unprotected SS surface with an area possibly larger than the original one. Therefore, the numerical value of the corrosion rate is larger than that measured for the bare SS samples, while the corrosion potential remains practically the same. This is in accordance with the values presented in Tables 1 and 2. Figure 8 shows a micrograph of such a coating showing the occurrence of cracks and the presence of small chromium oxide crystals. Furthermore, preliminary studies of some of the samples by Rutherford back scattering spectroscopy suggest that chromium diffusion into the coating layer is a process that already starts at temperatures as low as 450° C and is enhanced at higher temperatures and longer times of heat treatment [29].

4. Conclusions

The results of this work clearly indicate that thin coatings of $30TiO_2$–$70SiO_2$ deposited by sol–gel methods on 316L stainless steel act very efficiently as corrosion protectors in acid media. Thus, the measured corrosion rate drops by almost one order of magnitude in experiments carried out at 50° C in 15% H_2SO_4 solutions. The time and temperature used for the heat treatment during densification of the films proved to be important parameters for the performance and endurance of these coatings and have to be carefully controlled. Other related materials mentioned in the introduction section of this paper show similar behaviour to that of TiO_2–SiO_2 and should be further investigated.

Acknowledgements

This research was supported by FAPESP, FINEP, CNPq, CAPES/PICD and the Program RHAE–New Materials, Brazil.

References

[1] H. H. Uhlig and R. W. Revie, 'Corrosion and Corrosion Control', J. Wiley & Sons, New York (1985).
[2] D. A. Jones, 'Principles and Prevention of Corrosion', Maxwell-MacMillan (1992).
[3] L. L. Shreir, 'Corrosion', vol. 2, Newnes–Butterworths (1976).
[4] C. J. Brinker and G. W. Scherer, 'Sol–Gel Science: the Physics and Chemistry of Sol–Gel Processing', Academic Press, San Diego (1990).
[5] S. Sakka, *in* 'Sol–Gel Science and Technology' (edited by M. A. Aegerter, M. Jafelicci Jr., D. F. Souza and E. D. Zanotto) World Scientific, Singapore (1991), pp. 346–374.
[6] H. Schmidt, *in* 'Chemistry, Spectroscopy and Applications of Sol–Gel Glasses' (edited by R. Reisfeld and C. K. Jorgensen), Springer-Verlag, Berlin (1992) pp. 119–152.
[7] S. Sakka and T. Yoko, *in* 'Chemistry, Spectroscopy and Applications of Sol–Gel Glasses' (edited by R. Reisfeld and J. K. Jorgensen) Springer-Verlag, Berlin (1992) pp. 89–118.
[8] J. Schlichting and S. Neumann, *J. Non-Cryst. Solids* **48** (1982) 185.
[9] J. Martinsen, R. A. Figat and M. W. Schafer, *Mat. Res. Soc. Symp. Proc.* **32** (1984) 361.
[10] R. K. Brow and C. G. Pantano, *Mat. Res. Soc. Symp. Proc.* **32** (1982) 361.
[11] S. Ogiwara and K. Kinugawa, *Yogyo-Kyokai-Shi* (*in Japanese*) **90** (1982) 157.
[12] A. Matsuda, Y. Matsuno, S. Katagama, T. Tsuno, N. Tohge and T. Minami, *J. Ceram. Soc. Jpn., Int. Ed.* **100** (1992) 1079.
[13] O. Sanctis, L. Gomez, N. Pelligri, C. Parodi, A. Marajofsky and A. Duran, *J. Non-Cryst. Solids* **121** (1990) 338.
[14] N. Tohge, A. Matsuda and T. Minami, *J. Am. Ceram. Soc.* **70** (1987) C13.
[15] M. Guglielmi, D. Festa, P. C. Innocenzi, P. Colombo and M. Gobain, *J. Non-Cryst. Solids* **147 & 148** (1992) 474.
[16] A. R. Di Giampaolo, M. Puerta, J. Lira and N. Ruiz, *ibid.* **147 & 148** (1992) 467.
[17] M. Atik and M. A. Aegerter, *ibid.* **147 & 148** (1992) 813.
[18] M. Atik, C. R'kha and J. Zarzycki, *J. Mat. Sci. Lett.* **13** (1994) 266.
[19] M. Atik and M. A. Aegerter, *in* 'Better Ceramics Through Chemistry V', vol. 271 (edited by M. J. Hampden-Smith, W. G. Klemperer and C. J. Brinker) MRS, Pittsburg (1992) pp. 471–476.
[20] K. Izumi, H. Tanaka, Y. Uchida, N. Tohge and T. Minami, *J. Non-Cryst. Solids* **147 & 148** (1992) 483.
[21] M. Atik and J. Zarzycki, *J. Mat. Sci. Lett.* (1994), in press.
[22] M. Atik and M. A. Aegerter, submitted.
[23] P. Lima Neto, M. Atik, L. A. Avaca and M. A. Aegerter, *J. Sol–Gel Sci. & Tech.* **1** (1993) 177.
[24] M. Atik, P. Lima Neto, M. A. Aegerter and L. A. Avaca, Proc. 44th ISE Meeting, Berlin (1993).
[25] P. Lima Neto, M. Atik, L. A. Avaca and M. A. Aegerter, *J. Sol–Gel Sci. & Tech.* **2** (1994) 529.
[26] M. Atik, PhD thesis, University of Montpellier, France (1990).
[27] A. J. Sedriks, 'Corrosion of Stainless Steels', J. Wiley & Sons, New York (1979).
[28] J. O'M. Bockris and A. K. N. Reddy, 'Modern Electrochemistry', vol. 2, Plenum Press (1970).
[29] M. Atik, P. Lima Neto, J. C. Acquadro, L. A. Avaca and M. A. Aegerter, unpublished results.